

Shear on particles exposed to backswept mixing flow with a view to stress-sensitive cell response

S.D. Vlaev^{1*}, D. Georgiev²

¹*Institute of Chemical Engineering, Bulgarian Academy of Sciences, Acad. G. Bonchev Str., Bl. 103, 1113, Sofia, Bulgaria.*

²*Chemical Engineering Department, Bourgas University “Prof. Dr. A. Zlatarov”, 1 Boul. Prof. Yakimov, 8010 Bourgas, Bulgaria*

Received April 3, 2017; Accepted May 23, 2017

The flow impact over a spherical particle immersed in a biofluid at the impeller plane of a stirred laboratory bioreactor is examined. Based on the entire particle surface, the system mimics the flow effect upon living cells at growth being affected by hydrodynamic stress. Backswept (BS) circulation flow showed weak shear effect and was expected to stand as prospective operational means for growth in suspension cultures. A dual modified backswept impeller was selected to generate the flow circulation around the particle. Computational fluid dynamics (CFD) methodology was used. The shear distribution was obtained in the reactor inner volume as well as on the surface of the immersed body. The maximum wall-shear rate values were determined to be in the range from 1200 to 4000 s⁻¹. Evidence is given for areas of critical performance that imply cell damage in practical culture.

Keywords: mixing, backswept impeller, colloidal dispersions, wall shear, CFD

INTRODUCTION

The flow shear conditions near immersed particles in agitated bioreactors are important in biotechnology. Rapid deformations occur in many industrial systems, including cell and mycelia cultures in bioreactors for production of proteins, antibiotics, and other value added products. Cell fragmentations have been reported to be caused by such complications. Therefore, works devoted to hydrodynamic stress in mixing reactors and process strategies in relation to rotational speed and gassing present continuous interest [1]. Among these, the problem of cell negative response by the flow impact at shear conditions near immersed living particles in sparged cultures of agitated bioreactors prevails [2-7]. Shear has been identified as the cause of decreasing cell viability and morphology changes are frequently observed [8, 9]. Gas bubbles have been also reported to increase the shear stress around floating micro-objects [9]. In case of growth in micro-carrier cultures, loss of viable cells has been reported even at laminar stresses in the range of 0.5 to 10 Pa [10]. Referring to the overview of Nienow and coworkers [1], one finds that potential risks of cell damage lie within the specific flow field generated by the impeller and the performance of the gas flow related to bubble formation in the sparger zone, impeller discharge area and bubble bursting at the air-medium interface. In some cases, liquid jets (up to 5 m/s) are produced at gas cavities that may increase shear stress up to 100-300 Pa [11].

Considering the regions of potential risk for cell fragmentation in agitated reactors, namely, the sparger, the impeller discharge area, the vessel bulk bubble rise, it is of potential interest to reveal the value of shear force per unit surface acting on a particle in these zones.

In general, referring to the properties of impeller mixing of cell suspensions, one should avoid intensive high-shear conventional impellers. Recommendations for effective operation of sparged agitated bioreactors have been given [11]. Exemplifying animal cells, in order to avoid cell damage the impeller should be of a type that does not produce excessively high local rates of energy dissipation. Relatively large fluid-foil impellers, such as Elephant ear impeller [12] have been studied. Data on particle wall shear rates generated by radial flow conventional Rushton (RT) impellers [12, 13] and fluid-foil Narcissus [12] have been reported. RT showed high wall-shear rates critical for cells. In contrast, recent comparison of radial flow (RT) and backswept flow (BSF) impellers [14] has shown mild operating conditions in terms of shear in favor of the latter. It is expected that backswept impellers could be appropriate operational means for mixing and growth of stress-sensitive suspension culture. However, data on wall shear generated by backswept impellers on particles in bioreactors are lacking. In most cases, aeration of culture takes place and the effect of gassing in cases of BSF is also unknown.

In view of responding to engineering interest on a new BSF impeller, the aim of the study is to uncover the shear conditions in the flow over a

* To whom all correspondence should be sent:
E-mail: mixreac@gmail.com

particle exposed to the impact of BS impeller discharge and to compare these conditions with reference critical values in order to assess the flow properties of a relevant bioreactor operation.

The flow is a highly non-uniform one due to the impeller induced generic wide-spectrum velocity variation in stirred tanks, as well as due to the non-linearity of shear stress *vs.* shear deformation rate in agitated complex fluids. For that reason, the visualization technique based on CFD methodology was implemented as the most appropriate one for the analysis.

EXPERIMENTAL

Focusing on the physical model, the experimental reactor schematic is shown in Fig. 1. Addressing standard conditions in biological reactors, a dual impeller stirred Biostat vessel with tank diameter of 0.165 m and impeller diameter of 0.066 m (*Sartorius Biostat Aplus*) [15] was simulated (Fig.1). The working volume was 4.5 dm³. Impellers with modified curved arc-shaped blades [16] were used to generate the vessel backswept hydrodynamics. In cases, air was fed through a ring sparger with 12 one-mm openings. Further details on the system geometry have been reported elsewhere [14]. Interaction between flow and particles was included by assuming a single stagnant particle exposed to flow discharge driven by the rotating impeller, thus developing the strain corresponding to the maximum (i.e. relative between the fluid and the particle surface) velocity at the immersed body. For that purpose, a model sphere 5 mm in diameter was positioned in the impeller plane at a distance of 2 cm off the impeller tip opposing the discharge flow direction (Fig. 1). The shear parameters around and upon this probe were targeted.

The significance of fluid friction property for the fragmentation analysis was recognized and fluids of non-Newtonian flow properties frequent in practice were studied. The reference practical range of *S* for mixing of cell culture $\sim 10 \text{ s}^{-1}$ through 10 ks^{-1} was met by various rotational speeds *N*. Four prototype fluids corresponding to different states of the experimental biofluid [15] were simulated, the flow index *n* and consistency coefficient *K* varying as follows: $n=0.78, K=0.02 \text{ Pa}\cdot\text{s}^n$, $n=0.78, K=0.1 \text{ Pa}\cdot\text{s}^n$, $n=0.38, K=0.26 \text{ Pa}\cdot\text{s}^n$ and $n=0.34, K=0.55 \text{ Pa}\cdot\text{s}^n$.

The Metzner constant required to calculate the average shear rate for curved blades was 7.1, as reported determined by Taniyama and Sato [17] and reported in [18].

The study covers an apparent viscosity range less than 50 m Pa.s and relative aeration flow rate of 1 vvm that applies to a wide range of bioprocess technical scale conditions [15]. The flow pattern in small vessels is an intensive one and the corresponding Reynolds numbers for rotational flow of $0.5\text{-}1\cdot 10^4$ obtained assumed turbulent conditions.

Shear rate was determined by a numerical procedure using CFD model and solution methodology. The following details were worked out.

The flow field was simulated by the RANS standard *k-ε* (SKE) model and the Eu-Eu formulation of two-phase gas-liquid flow. For the moving volume the multiple reference frame approach [19] was used.

The hydrodynamic stress was determined from the shear rate (\dot{S}) and the constitutive equation of the fluid (non-Newtonian power law one):

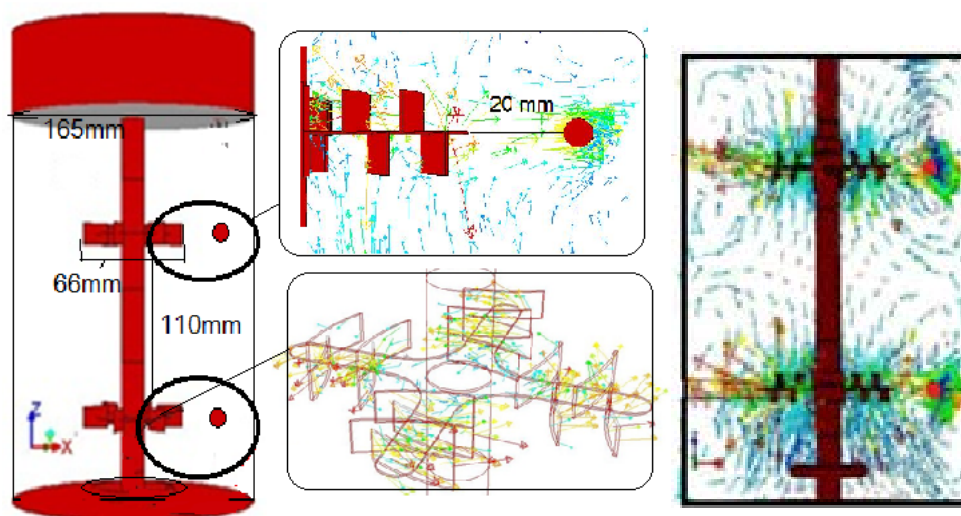


Fig.1. Reactor, impeller and spherical probe schematic and flow patterns observed.

$$\dot{S} = \frac{\partial V_j}{\partial x_i} + \frac{\partial V_i}{\partial x_j} \quad (1)$$

$$\tau = K\dot{S}^n \quad (2)$$

$$\mu_a = K \left(\frac{\partial V_j}{\partial x_i} + \frac{\partial V_i}{\partial x_j} \right)^{n-1} \quad (3)$$

In equations (1-3) V indicates local velocity, τ is shear stress, μ_a is apparent viscosity.

The governing equations [19] were solved numerically by Fluent (*ANSYS FLUENT Release 13.0, ANSYS, Inc., 2010*). The computational grid was generated by using Gambit (version 2.1). Unstructured mesh for complex shape with approx. 10^5 cells tetrahedral mesh for the volumes next to the impeller blades and the probe and hexahedral mesh for the rest of the tank was used. The grid interface between the inner rotating cylindrical volume and the outer stationary volume was a conformal one. Mesh refinement degrees down to <0.05 mm linear dimension were generated in order to achieve near-surface velocity gradients.

The boundary conditions for the single phase case were symmetry for the bed top and no-slip for wall boundaries in single phase flow and air velocity inlet and pressure outlet for the gas phase in cases of two-phase gas-liquid flow. A steady solution was performed for the single phase cases and a transient one for the presence of gas. The convergence criterion was set for the velocities and turbulence values equal to 1×10^{-6} . Reasonable convergence was achieved. Validation was carried out by basic parameters, momentum, power number, as well as by comparing values of experimental and predicted wall shear rates. The simulation in this format has been experienced formerly for radial flow and its validation related to non-Newtonian flow has been reported [12].

RESULTS AND DISCUSSION

Assuming that cell fragmentation is proportional to the slip velocity of fluid-particle interaction, shear rate on particle \dot{S}_p was selected as the representative parameter of interest. However, overall shear rate (\dot{S}) distribution, including bulk fluid shear \dot{S}_f was also examined. Answers of three basic issues were sought: (1) How much is the extent of inner fluid shear rate \dot{S}_f and the corresponding particle wall shear rate \dot{S}_p generated by the BS impeller-imposed

flow; (2) Is the effect of gas presence a significant one; (3) Within the practical range of input power, could the flow produce shear stress values τ_p critical for processing of mycelia or animal cells?

The flow pattern caused by backswept flow is a small loop radial one, as illustrated in **Fig. 1**. Thus, the impeller zone facing the particles was of major interest.

Both fluid shear rate and particle wall shear were target values and the vessel bulk and particle surface were examined. Accordingly, tank-scale and particle-scale data are illustrated, the first ones showing the flow field and its zones of spread in 2-D vertical plane ($x=y$) passing through the particle (**Fig. 2**) and in radial $X-Y$ plots along a tangent and a central line adhering and passing through the particle, respectively (**Figs. 3, 4**); The second scale visualized the near-wall shear distribution directly as a solid body representation of particle surface (**Fig. 5**). **Figs. 2-5** and **Tables 1-2** contain the results.

Fig. 2 illustrates the typical flow field for the case of backswept flow in both 2-D zones of spread and average zone shear rate (in s^{-1}) at the two degrees of a non-Newtonian flow, i.e. low consistency ($K=0.02$ Pa.sⁿ) and high consistency ($K=0.1$ Pa.sⁿ) one. Impeller speed $N=750$ rpm was selected as the most representative for the configuration of the dual arch-shaped impeller employed. The choice was based on previous comparative analysis with conventional BIostat showing equal reaction effectiveness of the conventional Rushton (RT) radial flow impeller at 400 rpm and the present one at 750 rpm relevant to a biological system producing exopolysaccharides [15]. The contour plots in the figure correspond to increasing deviation from Newtonian flow properties at no gas and gassed conditions. As illustrated, the bulk fluid shear rate \dot{S}_f , generated by the backswept impeller, is of the order of magnitude reported for conventional impellers, namely $<2 \cdot 10^2$ s^{-1} [20, 21]. As estimated by the spread of zone ($\dot{S}_f \sim 10$ s^{-1}), \dot{S}_f is getting damped successively by rising consistency and gas introduction.

Shear distribution along selected lines, i.e. a central one and a tangent one, is shown in **Figs. 3** and **4**. Both upper and lower impeller zone were examined and showed similar patterns; the results in the figures represent the upper impeller and particle zone. **Fig. 3** shows the effect of mixing intensity controlled by rpm and consistency at no gas conditions. Point values of maximum shear \dot{S}

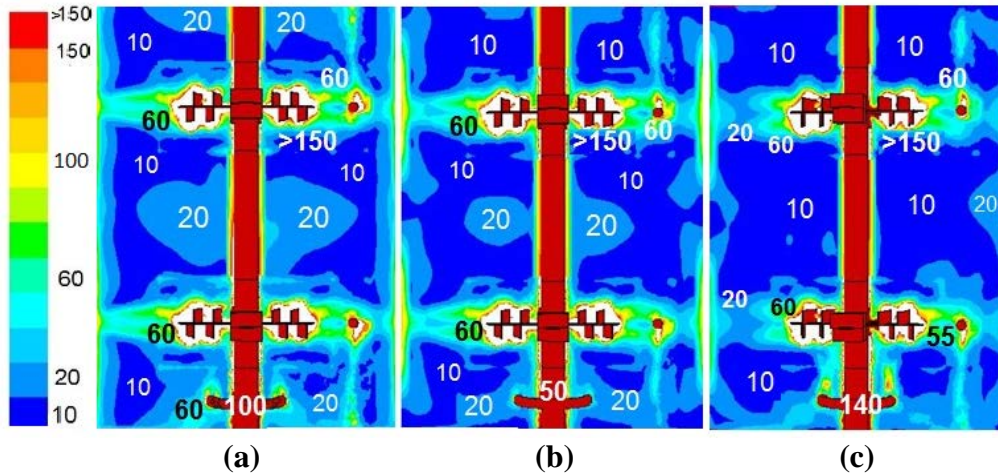


Fig. 2. Typical 2-D image of the vessel bulk fluid shear rates (s^{-1}) at $N=750$ rpm and increasing deviation from Newtonian properties at no gas and gassed conditions: (a) fluid $n=0.78/K=0.02$ Pa.sⁿ, no gas, (b) fluid $n=0.78/K=0.1$ Pa.sⁿ, no gas, (c) fluid $n=0.78/K=0.1$ Pa.sⁿ, gassed.

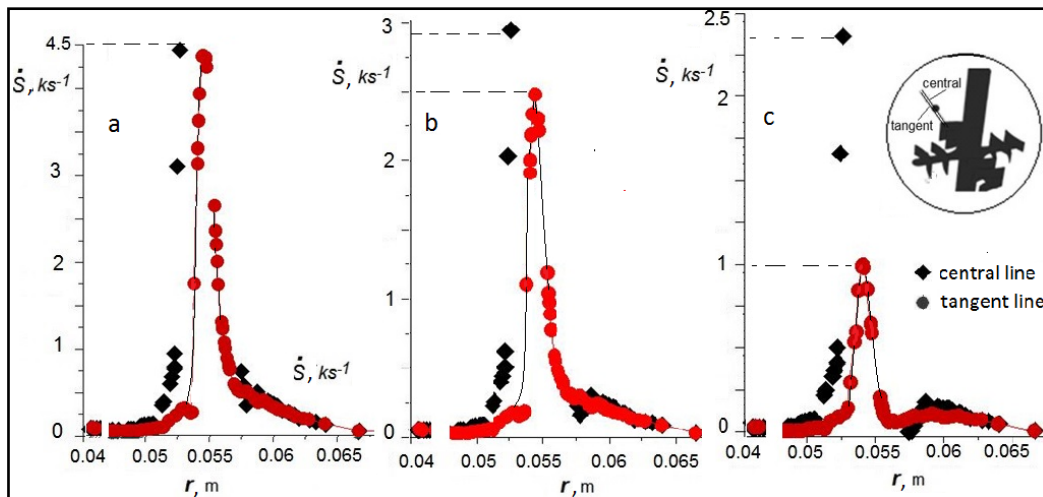


Fig. 3. Effect of rpm and consistency on shear rates ($\dot{\gamma}$) generated by backswept flow at no gas conditions: $\dot{\gamma}$ versus radial position along the central (◆) and tangent (●) lines (a) $N=1080$ rpm, $n=0.78$, $K=0.02$ Pa.sⁿ (b) $N=750$ rpm, $n=0.78$, $K=0.02$ Pa.sⁿ, and (c) $N=750$ rpm, $n=0.78$, $K=0.1$ Pa.sⁿ

corresponding to the radial locations near particle surface, e.g. frontal and tangent ones, are seen; only the radial interval around the particle ($0.04 < r < 0.068$, $0.053 < r_p < 0.058$) is shown. Fig. 3(a) versus 3(b) shows the rpm effect, while Fig. 3(b) vs. Fig. 3(c) shows the effect of fluid consistency. One estimates that the maximum particle wall shear rate imposed by BS flow is of the order of 1000 to 4500 s^{-1} . In parallel, mixing intensity shows strong impact on shear, i.e. 30 % speed deviation (18 rps to 12.5 rps) might cause a 2-fold particle shear decrease (between 4.5 and 2 ks^{-1}). Comparing the $\dot{\gamma}$ -profiles of a moderately viscous fluid (~ 7 mPa.s, $K=0.02$ Pa.sⁿ) and a highly viscous fluid (~ 37 mPa.s, $K=0.1$ Pa.sⁿ) at similar mixing intensity ($N=750$ rpm), the shear deformation rate decrease is obvious.

Fig. 4 shows the effect of gas presence at low ($K=0.02$ Pa.sⁿ) and high consistency ($K=0.1$ Pa.sⁿ).

The case of low consistency corresponding to low apparent viscosity (~ 7 mPa.s) at 900 rpm indicates sharp decrease of shear rate more than 30 % in gas presence. In contrast, (Fig. 3c and Fig. 4c compared), shear rate at high consistency corresponding to 5-fold viscosity rise is only slightly affected by gas presence and shows no shear increase or only slight increase, e.g. 7%, possibly due to the increase of fluid mobility in parallel to the intensified motion caused by the gas bubbles.

In Figs. 5(a) and 5(b) shear rate zonal spread on the particle surface is revealed. In both figures particle wall-shear $\dot{\gamma}_p$ (in ks^{-1}) is illustrated. Extreme non-uniformity of shear, as well as zones of maximum shear showing different spread over particle side and rear are registered. Inferring on the effects seen in the figure, the high stress zone is expected by the side stream, while the lowest stress

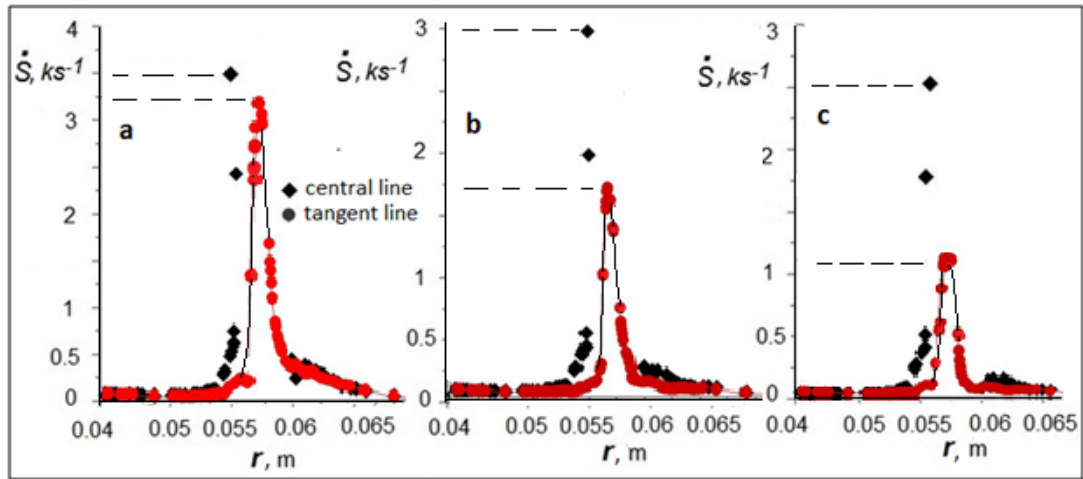


Fig. 4. Effect of gas on shear rate (ks^{-1}) generated by backswept flow at low and high consistency: \dot{S} versus radial position along the central (\blacklozenge) and tangent (\bullet) lines at: no gas, $N=900$ rpm, $K=0.02 \text{ Pa}\cdot\text{s}^n$, $n=0.78$, (b) with gas, $N=900$ rpm, $n=0.78$, $K=0.02 \text{ Pa}\cdot\text{s}^n$, (c) with gas, $N=750$ rpm, $n=0.78$, $K=0.1 \text{ Pa}\cdot\text{s}^n$,

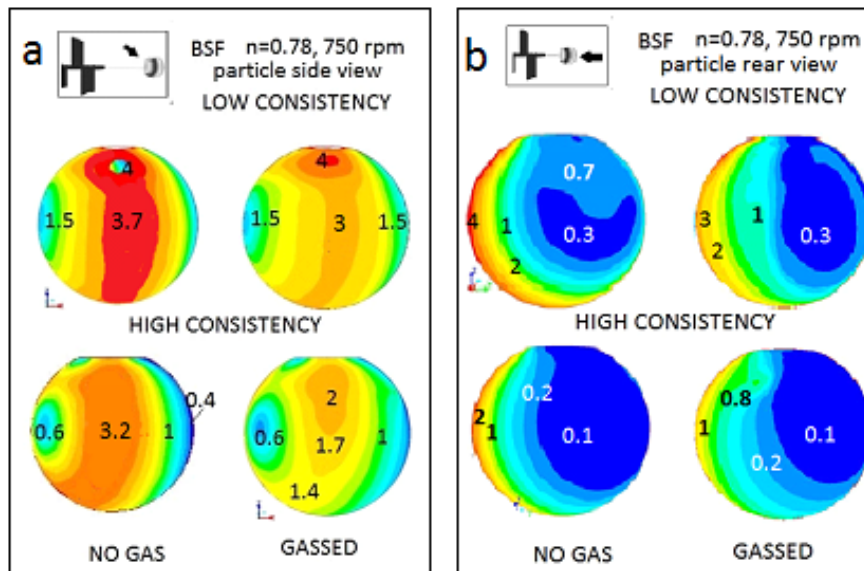


Fig.5. Solid body image of \dot{S}_p - zonal spread ($\dot{S}_p \cdot 10^3 \text{ s}^{-1}$) at backswept flow (BSF): \dot{S} - distribution at 750 rpm corresponding to low ($K=0.02 \text{ Pa}\cdot\text{s}^n / n=0.78$) and high ($K=0.1 \text{ Pa}\cdot\text{s}^n / n=0.78$) consistency, gas absence and presence in (a) particle side view, and (b) particle rear view

zone in gas presence coincides with the low pressure gas filled zone at the particle rear. This is valid strongly for the case of low consistency ($K=0.02 \text{ Pa}\cdot\text{s}^n$).

Figs. 3-5 present local \dot{S} - values. Based on the cross-sectional area of the plane ($x=y$) and the particle considered, surface-area averaged values corresponding to the various performance variables were determined. Table 1 contains the summary of results. In the Table, the values of shear stress are determined and the opposite effect of gas on shear at low and high consistency is registered. The data allow comparison between cases of backswept flow (BSF) and other flow types, e.g. generated by radial flow by Rushton (RT) impeller. Table 2 compares

the cases' parameters including data for flat-blade (RT) impeller mixing [12] based on specific input power, i.e. power P per unit fluid volume V_r . Referring to a similar range of input power, e.g. $1-6 \text{ W}/\text{dm}^3$, particle wall shear imposed by a conventional flat-blade impeller RT is about 3-fold higher than the one determined for the backswept impeller studied.

While showing the magnitude and the effects, it is the practical outcome of the result that is important: what are the ranges of shear stress imposed on a stagnant particle in configuration of backswept flow and how they conform to reported criteria for cell damage? The results in Tables 1 and 2 suggest the answer.

Table 1 Average wall shear stress: the effect of gassing

Fluid	N [rpm]	Gas U/G	μ_a [mPa s]	Re_m [-]	\dot{S}_f [s ⁻¹]	\dot{S}_p [s ⁻¹]	τ_p [Pa]
$n=0.78$ $K=0.02 \text{ Pa}\cdot\text{s}^n$	600	U*	7.8	5680	43.9	1680	6.6
		G			41.5	1530	6.1
	750	U	7.5	7700	56.6	2360	8.55
		G			50.7	1950	7.4
	900	U	7.3	9200	67.3	3000	10.3
		G			54.6	1940	7.3
	1080	U	6.9	11600	75.6	3900	12.6
		G			67.7	2720	9.6
$N=0.78$ $K=0.1 \text{ Pa}\cdot\text{s}^n$	750	U	37.4	1600	47.2	1220	25.5
		G			48.5	1330	27.3

*Conditions: U *ungassed*, G *gassed***Table 2** Comparison of shear imposed by the backswept (BS) and Rushton (RT) impellers

Flow Pattern	N [rps]	P/V_r [Wdm ⁻³]	\dot{S}_f [s ⁻¹]	\dot{S}_p [ks ⁻¹]	τ_p [Pa]
BSF	10	1.7	43.9	1.68	6.1
	12.5	3.3	56.6	2.36	8.5
	15	5.7	67.3	3.0	10.3
RT [12]	6.7	1.4	24.5	9.57	25.4
	10	4.6	36.7	9.64	25.6

Recalling critical values of shear stress likely to cause damage to animal cells or mycelia reported in the literature, the relevant flow conditions could be classified in terms of shear inducing properties as appropriate or non-appropriate for the specific operation.

Critical values for cell damage have been reported in the literature [1-9]. Animal cell damage was found to start in the range of shear stress from 0.2-200 Pa [2]. Recent studies pointed at threshold values of hydrodynamic stress of ~25-30 Pa [6]. Studies related to the performance of *Carthamus tinctorius* L. by Liu *et al.* [7] showed that changing shear stress between 10 and 50 Pa, the specific death rate of the plant cells increased 5-fold. They confirmed the previous result [3] that significant cell damage of plant cells occurred when the maximum shear stress exceeded 70 Pa. In case of growth in microcarrier cultures, loss of viable cells has been reported even at laminar stresses in the range 0.5 to 10 Pa [10]. Referring to living microobjects, studying the effect of hydrodynamic stress on the growth of *Xanthomonas campestris* cells, Garcia-Ochoa *et al.* [8] reported morphology changes yet at 9 Pa and a 40 % decrease of cell viability at shear stress of 35 Pa.

Based on these data, one could realize that a vessel could operate at a mixing regime generating particle shear stress exceeding 70 Pa at an increased degree of risk for damage in case of shear-sensitive

biomass. Nevertheless, to avoid detrimental effects shear deformation rate should not exceed ~3 ks⁻¹ and shear stress ~10 Pa. Referring to the typical range of mixing variables in Table 2, the backswept induced circulation studied is well within the limits for bioprocessing. The analysis based on the results points at the range of moderate rotational motion generated by the backswept unit at lower rotational speed, e.g. less than 900 rpm to be the most appropriate one for feasible operation involving cell culture. Operational modes exceeding 10 Pa could be acceptable for bioreactors processing mycelia biomass with a danger of some loss of activity.

CONCLUSIONS

In conclusion, the study presents a CFD-based assessment of an important flow parameter - an image of shear imposed on particles immersed in a complex non-Newtonian fluid with a view to engineering application to suspension culture of stress-sensitive cells in stirred bioreactors. It reveals the maximum flow impact at the wall of a stagnant particle in colloidal dispersion circulated by means of a backswept impeller. The rates of shear generated by the radial velocity-dominated circulation flow, as well as the hydrodynamic shear stress on particles at no gas conditions and in gas presence are determined. Evidence is given for areas of critical performance in a case of primary circulation that imply changes in cell physiological response in

practical cases of culture bioprocessing. Referring to reported critical shear stress values in the literature, the data for backswept flow allow extension of classification of practically occurring operational regimes in terms of potential risks for cell damage.

Acknowledgement: This article is based upon work from European Cooperation in Science and Technology (COST) Action MP1305, supported by COST.

REFERENCES

1. A. Amanullah, B.C. Buckland, A. W. Nienow, in: Handbook of Industrial Mixing. E.L. Paul, V.A. Atiemo-Obeng, S.M. Kresta (eds), Wiley, New Jersey, 2004, Ch. 18.
2. L. Van der Pol, J. Tramper, *Trends Biotechnol.*, **16**, 323, 1998.
3. D.D. Sowana, D.R.G. Williams, E.H. Dunlop, B.B. Dally, B.K. O'Neill, D.F. Fletcher, *Trans. Inst. Chem. Eng.*, **79A**, 867 (2001).
4. E.V. Guseva, N.V. Menshutina, J. Boudrant, J., in: Proc. 15th Eur. Conf. on Mixing, R. Abiev (ed.), S. Petersburg State Inst. Technol., S. Petersburg, 2015, p. 134.
5. Th. T. Tran, W.R. Hwang, in: Proc. 15th Eur. Conf. on Mixing, Abiev, R. (ed.), S. Petersburg State Inst. Technol., S. Petersburg, 2015, p. 345.
6. B. Neunstoecklin, M. Stettler, Th. Solacroup, H. Broly, M. Morbidelli, M. Soos, *J. Biotechnol.*, **194**, 100 (2015).
7. Yu Liu, Z.J. Wang, J. Xia, C. Haringa, Y. Liu, J. Chu, Y.P. Zhuang, S.L. Zhang, *Biochem. Eng. J.*, **14**, 209 (2016).
8. F. Garcia-Ochoa, E. Gomez, A. Alcon, V.F. Santos, *Bioprocess Biosyst. Eng.*, **36**, 911 (2013).
9. S.J. Meier, T.A. Hatton, D.I.C. Wang, *Biotechnol. Bioeng.*, **62**, 468 (1999).
10. J.G. Aunins, H.J. Henzler, in: Biotechnology 2nd Edn, (Vol. 3, Bioprocessing), H.J. Rehm, G. Reed (eds.), VCH, Weinheim, 1993.
11. Y. Chisti, *Trends Biotechnol.*, **18**, 420, 2006.
12. S.D. Vlaev, I. Nikov, M. Martinov, *Chem. Eng. Sci.*, **61**, 5455 (2006).
13. C.C. Bustamante, W.O. Cerri, A.C. Badino, *Chem. Eng. Sci.*, **90**, 82 (2013).
14. S.D. Vlaev, D. Georgiev, in: Scientific Works of University of Food Technologies vol. 61, University of Food Technologies, Plovdiv, 2014, 745.
15. S.D. Vlaev, S. Rusinova-Videva, K. Pavlova, M. Kuncheva, I. Panchev, S. Dobрева, *Appl. Microbiol. Biotechnol.*, **97**, 5303 (2013).
16. S. Kraitshev, S.D. Vlaev, V. Lossev, P. Staykov, *Biotechnol. Biotechnol. Eq.*, **15**, 128 (2000).
17. I. Taniyama, T. Sato, *Kagaku Kogaku*, **29**, 709 (1965).
18. S. Nagata, *Mixing Principles and Applications*, Wiley, New York, 1975.
19. V.V. Ranade, *Computational flow modeling for chemical reactor engineering*, Academic Press, London, 2002.
20. R. R. Hemrajani, G. B. Tatterson, in: Handbook of Industrial Mixing (Eds. E.L. Paul, V.A. Atiemo-Obeng, S.M. Kresta), Wiley, New Jersey, 2004, Ch. 6.
21. K. Van't Riet, J.M. Smith, *Chem. Eng. Sci.*, **30**, 1093 (1975).

СКОРОСТИ НА СРЯЗВАНЕ ВЪРХУ ЧАСТИЦИ ПРИ РАЗБЪРКВАНЕ С ДЪГООБРАЗНИ ЛОПАТКИ СЪС ЗНАЧЕНИЕ ЗА ФИЗИОЛОГИЯТА НА МИКРООРГАНИЗМИ ЧУВСТВИТЕЛНИ КЪМ МЕХАНИЧНО НАПРЕЖЕНИЕ

С.Д. Влаев Д. Георгиев

Институт по инженерна химия, БАН, ул. Акад. Г. Бонев бл. 103, София 1113, България
Бургаски университет „Проф. Асен Златаров“, кат. „Инженерна химия“, бул. Проф. Якимов, 1, Бургас 8010, България

Получена на 3 април, 2017 г.; приета на 23 май, 2017 г.

(Резюме)

Изследвано е влиянието на хидродинамиката на разбъркване върху сферична частица, потопена във флуид в равнината на импелер с реактивни дъгообразни лопатки. Системата наподобява влияние на поток върху живи клетки на микроорганизми в биореактори с разбъркване. Импелерът с реактивни лопатки осигурява понижено механично напрежение и е перспективен за приложение във ферментатори със суспендирани микроорганизми. Приложена е методика на компютърна изчислителна хидродинамика. Получени са 2-D и 3-D разпределения на скоростта на срязване в обема на флуида и върху повърхността на потопеното тяло. Установени са максимални стойности на повърхностната скорост на срязване в интервала 1200-4000 сек⁻¹. Показани са зони на тангенциална деформация, които могат да се окажат критични за физиологията на клетки на микроорганизми, чувствителни към механично въздействие.